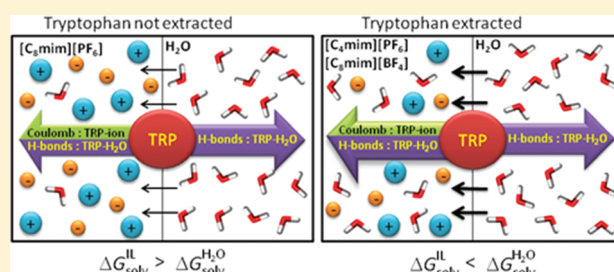


# Extraction of Tryptophan with Ionic Liquids Studied with Molecular Dynamics Simulations

Abirami Seduraman,<sup>†</sup> Ping Wu,<sup>§</sup> and Marco Klähn<sup>\*,†,‡</sup><sup>†</sup>Institute of High Performance Computing, 1 Fusionopolis Way, 16-16, Connexis, Singapore 138632, Republic of Singapore<sup>‡</sup>Technische Universität München, Physik-Department, T38, James-Frank-Strasse 1, 85748 Garching, Germany<sup>§</sup>Singapore University of Technology and Design, 20 Dover Drive, Singapore 138682, Republic of Singapore Supporting Information

**ABSTRACT:** Extraction of amino acids from aqueous solutions with ionic liquids (ILs) in biphasic systems is analyzed with molecular dynamics (MD) simulations. Extraction of tryptophan (TRP) with the imidazolium-based ILs [C<sub>4</sub>mim][PF<sub>6</sub>], [C<sub>8</sub>mim][PF<sub>6</sub>], and [C<sub>8</sub>mim][BF<sub>4</sub>] are considered as model cases. Solvation free energies of TRP are calculated with MD simulations and thermodynamic integration in combination with an empirical force field, whose parametrization is based on the liquid-phase charge distribution of the ILs. Calculated solvation free energies reproduce successfully all observed experimental trends according to the previously reported partition of TRP between water and IL phases. Water is present in ILs as a cosolvent, due to direct contact with the aqueous phase during extraction, and is found to play a major role in the extraction of TRP. Water improves solvation of cationic TRP by 7.8 and 5.1 kcal/mol in [C<sub>4</sub>mim][PF<sub>6</sub>] and [C<sub>8</sub>mim][PF<sub>6</sub>], respectively, which is in the case of [C<sub>4</sub>mim][PF<sub>6</sub>] sufficient to extract TRP. Extraction in [C<sub>8</sub>mim][PF<sub>6</sub>] is not feasible, since the hydrophobic octyl groups of the cations limit the water concentration in the IL. The solvation of cationic TRP is 2.4 kcal/mol less favorable in [C<sub>8</sub>mim][PF<sub>6</sub>] than in [C<sub>4</sub>mim][PF<sub>6</sub>]. Water improves the solvation of TRP in ILs mostly through dipole–dipole interactions with the polar backbone of TRP. Extraction is most efficient with [C<sub>8</sub>mim][BF<sub>4</sub>], where hydrophilic BF<sub>4</sub><sup>−</sup> anions substantially increase the water concentration in the IL. Additionally, stronger direct electrostatic interactions of TRP with BF<sub>4</sub><sup>−</sup> anions improve its solvation in the IL further. The solvation of cationic TRP in [C<sub>8</sub>mim][BF<sub>4</sub>] is 3.4 kcal/mol more favorable than in [C<sub>8</sub>mim][PF<sub>6</sub>]. Overall, the extractive power of the ILs correlates with the water saturation concentration of the IL phase, which in turn is determined by the hydrophilicity of the constituting ions. The results of this work identify relations between the extraction performance of ILs and the basic chemical properties of the ions, which provide guidelines that could contribute to the design of improved novel ILs for amino acid extraction.



## 1. INTRODUCTION

Amino acids are the basic constituents of proteins and play a key role in several biological processes. Amino acids are of high relevance for the food industry, where, e.g., lysine, tryptophan, and methionine are used as additives in animal fodder to improve nutritional quality.<sup>1</sup> Furthermore, glutamates, serine, and aspartic acid are also used as taste enhancers and seasoning agents.<sup>2</sup> A variety of amino acids are also used in the pharmaceutical industry to prepare intravenous nutrient solutions.<sup>3,4</sup> Although most of the amino acids can be obtained by the fermentation method, their separation from the fermentation broth is quite difficult.<sup>5,6</sup> Various extraction techniques have been explored, where extraction from liquid–liquid biphasic systems have been recognized as the most promising method.<sup>7,8</sup> This technique has been widely applied owing to its effectiveness, simple implementation, low cost, and ease of scale up. However, in liquid–liquid extraction processes, typically toxic, flammable, and volatile organic compounds have been used as extractors, which raises environmental concerns. Furthermore, some amino acids are markedly hydrophilic, which impedes extraction with organic

solvents. Therefore, lipophilic ion extractants as well as other hydrophobic counterions have been added to the organic solvents to enhance the extractive power.<sup>9–16</sup> However, Smirnova et al. reported that the presence of crown ether, for instance, is not sufficient to extract amino acids, so the anionogenic extractants dinonylnaphthalenesulfonic acid and di(2-ethylhexyl)phosphoric acid (D2EHPA) were added.<sup>17</sup> Even in these cases, complete extraction of the most hydrophilic amino acids could not be accomplished.

Ionic liquids (ILs) have been recently identified as a promising alternative to organic solvents for various applications. ILs are molten salts with melting points below 100 °C and are typically composed of asymmetric organic cations (such as imidazolium, pyridinium, and quaternary ammonium, for instance) and compact inorganic anions. These constituting ions can be varied independently to provide task-specific materials for specific

Received: July 15, 2011

Revised: November 22, 2011

Published: December 02, 2011

applications. Their remarkable intrinsic physicochemical properties such as excellent solvation properties, negligible vapor pressure, nonflammability, high thermal stability, and biocompatibility suggest ILs for a wide range of applications.<sup>8,18–23</sup> In particular, ILs have been proposed as an environmentally benign liquid–liquid extractant for organic compounds, which has been demonstrated by Rogers et al. in a pioneering work.<sup>24</sup> Since then, ILs have been used successfully to extract efficiently metal ions, organic compounds, as well as various biomolecules such as amino acids, proteins, carbohydrates, lactic acids, antibiotics, and alkaloids.<sup>24–39</sup>

Successful recovery of amino acids from pharmaceutical samples and fermentation broths with the IL 1-butyl-3-methylimidazolium hexafluorophosphate [C<sub>4</sub>mim][PF<sub>6</sub>] with crown ether dicyclohexano-18-crown-6 has been reported.<sup>34</sup> In contrast to organic solvents, this IL extracted even the most hydrophilic amino acids without addition of other ions. Furthermore, it was demonstrated that also other hydrophobic ILs, such as [C<sub>6</sub>mim][PF<sub>6</sub>], [C<sub>6</sub>mim][BF<sub>4</sub>], and [C<sub>8</sub>mim][BF<sub>4</sub>], successfully recovered amino acids from aqueous solutions.<sup>40–42</sup> These ILs do not mix with water and form biphasic systems, so that amino acids can be extracted from the aqueous phase into the ILs. The required water immiscibility of ILs depends sensitively on the ion composition of the IL. In a preceding work, we recently proposed a method to predict the water miscibility of novel ILs, which merely relies on ion size and ion charge distribution.<sup>43</sup> In any event, it was found that the performance of amino acid extraction in IL–water systems is sensitive to the pH value of the aqueous solution as well as the hydrophobic character and chemical structure of ions in the IL.<sup>40–42</sup> In particular, anion hydrophobicity and cation alkyl chain length were found to be dominating factors that influence the effectiveness of the extraction process.<sup>42</sup> Nevertheless, the molecular origin of these observations has not been elucidated. Considering the virtually infinite number of possible ion combinations in ILs, an *a priori* prediction of the extractive performance of novel ILs, which could be facilitated by such insights, would be highly desirable.

The aim of the present work is to study the underlying molecular mechanism that enables ILs to extract amino acids from aqueous solutions. Solvation free energies of tryptophan (TRP), solvated in various imidazolium-based ILs, were determined with molecular dynamics (MD) simulations to identify the factors that determine the extractive power of ILs. L-Tryptophan, which consists of the polar amine and carboxylic acid groups as well as of a mostly nonpolar indole side chain, is an essential amino acid in human diet and a precursor of the neurotransmitter serotonin. TRP was chosen as a model case because various IL–water partition coefficients,  $P_{\text{IL}/\text{W}}$ , have been measured that enabled a comparison with simulation results. In these measurements,  $P_{\text{IL}/\text{W}}$  values depend strongly on the pH values of the aqueous phase, where extraction occurred only at pH values that were substantially lower than the first dissociation constant of TRP ( $\text{p}K_1 = 2.38$ ). This means that only the fully protonated, i.e., cationic form of TRP was extracted. Hence, only extraction of cationic tryptophan (TRPc) was considered; however, the zwitterionic form (TRPz) was taken into account as a reference when necessary. Structures of the different protonation states of TRP are shown in Figure 1. In simulations considered ILs include 1-octyl-3-methylimidazolium paired with hexafluorophosphate, [C<sub>8</sub>mim][PF<sub>6</sub>], and tetrafluoroborate, [C<sub>8</sub>mim][BF<sub>4</sub>], to study the influence of anions on TRP extraction as well as 1-butyl-3-methylimidazolium hexafluorophosphate, [C<sub>4</sub>mim][PF<sub>6</sub>], to investigate the influence of the alkyl chain length. Furthermore, to

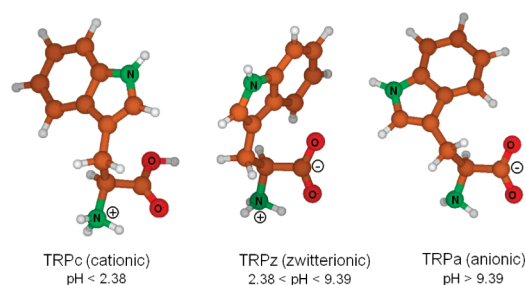


**Figure 1.** Representative structures of tryptophan in three different protonation states together with the range of pH values in which their occurrence dominates in water.

analyze the effect of water as a cosolvent in ILs on extraction of TRP, [C<sub>4</sub>mim][PF<sub>6</sub>] was simulated in the presence and absence of water in the IL. Taking water as a cosolvent into account is essential, since even hydrophobic ILs are hygroscopic so that direct contact with water in biphasic systems leads to diffusion of water into the IL phase until a saturation concentration is reached. These saturation concentrations have been measured previously.<sup>44</sup>

All simulations were performed with MD simulations and an empirical molecular mechanical (MM) force field for ILs that was developed in our preceding work.<sup>43,45</sup> Structural analysis was subsequently performed to gain insights into the coordination between water, ions, and the TRP solute. Free energy changes for the transfer of TRP between two ILs are calculated and compared with measured values that are derived from  $P_{\text{IL}/\text{W}}$  values. Finally, the effect of anions, alkyl chain length, and water on the solvation free energy of TRP is evaluated to identify the factors that determine the extraction performance of ILs.

## 2. METHODOLOGY

**2.1. Applied Force Fields.** Potential energies of simulated systems were calculated with the MM force field using a standard functional form

$$\begin{aligned}
 E_{\text{pot}}^{\text{MM}} = & \sum_{i,j}^{\text{bonds}} k_{ij}(l_{ij} - l_{0,ij})^2 + \sum_{i,j,k}^{\text{angles}} k_{ijk}(\phi_{ijk} - \phi_{0,ijk})^2 \\
 & + \sum_{i,j,k,l}^{\text{improper}} k_{ijkl}(\theta_{ijkl} - \theta_{0,ijkl})^2 \\
 & + \sum_{i,j,k,l}^{\text{torsions}} E_{ijkl}(1 + \cos(n_{ijkl}\phi_{ijkl} - \delta_{0,ijkl})) \\
 & + \sum_{i,j} \frac{q_i q_j e^2}{4\pi\epsilon_0 r_{ij}} + 4\epsilon_{ij} \left[ \left( \frac{\sigma_{ij}}{r_{ij}} \right)^{12} - \left( \frac{\sigma_{ij}}{r_{ij}} \right)^6 \right] \quad (1)
 \end{aligned}$$

A detailed description of eq 1 and used symbols can be found, e.g., in ref 45. The force field for [C<sub>4</sub>mim][PF<sub>6</sub>] was parametrized in our previous work,<sup>43</sup> while the force field for the other two considered ILs, [C<sub>8</sub>mim][PF<sub>6</sub>] and [C<sub>8</sub>mim][BF<sub>4</sub>], is described below. Bonded interactions for all simulated ILs were taken from the IL force field from Lopes et al.<sup>46</sup> TRP solutes were simulated with the AMBER-03 force field, whose suitability for the simulation of amino acids has been amply demonstrated.<sup>47</sup> Water molecules were described with the five-site potential TIPSP,<sup>48,49</sup>

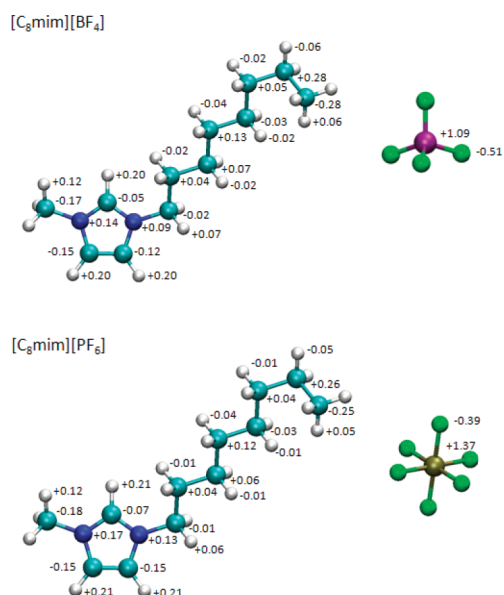


**Figure 2.** Atomic partial charges for ions that constitute  $[\text{C}_8\text{mim}][\text{BF}_4]$  and  $[\text{C}_8\text{mim}][\text{PF}_6]$ . Partial charges are based on the electrostatic potential of the ions (ESP charges) in the liquid phase using the CHELPG scheme.<sup>56</sup> Charges of chemically equivalent atoms were averaged. Partial charges are given in units of the elementary charge.

which was preferred over the widely used TIP3P<sup>50</sup> model, since evidence was found that TIP3P tends to overestimate water–ion interaction strengths.<sup>43,51</sup>

The IL force fields are based on the electron charge distribution in the actual liquid, in contrast to a conventional parametrization, where merely isolated ions or ion pairs have been considered as models for the liquid. In our previous work, we demonstrated that charge transfer between ions and IL induced charge polarization of single ions strongly influenced the energetic and dynamic properties of ILs.<sup>45,52</sup> An average electron charge transfer from cations to anions for the ILs  $[\text{C}_4\text{mim}][\text{BF}_4]$  and  $[\text{C}_4\text{mim}][\text{PF}_6]$  of 0.05 and 0.03 e, respectively, has been determined in a preceding work.<sup>43</sup> By neglecting the influence of the alkyl chain length on charge transfer the same values could be used for  $[\text{C}_8\text{mim}][\text{BF}_4]$  and  $[\text{C}_8\text{mim}][\text{PF}_6]$ , i.e., ions were parametrized with a total charge of  $\pm 0.95$  e and  $\pm 0.97$  e, respectively. While the average charge distribution in  $[\text{C}_4\text{mim}][\text{PF}_6]$  can be found in Figure 1 of ref 43, the charge distribution for the other two considered ILs had to be determined in the present work. Partial charges for  $[\text{C}_8\text{mim}][\text{BF}_4]$  and  $[\text{C}_8\text{mim}][\text{PF}_6]$  were derived with a QM/MM approach, in which the classical MD software GROMACS was coupled with the ab initio code Gaussian.<sup>53</sup> In this approach, one ion was treated with DFT using the B3LYP functional with a 6-31+g(d) basis set, while the surrounding liquid was described with the MM force field.<sup>54,55</sup> After an energy minimization of the hybrid potential, partial charges of the ion were determined with the CHELPG scheme.<sup>56</sup> Final partial charges were calculated as averages over a sample of 10 different ions in the IL, which were chosen successively as QM fragments. In the last step, these partial charges were scaled with the total ion charge to accommodate the previously determined charge transfer given above. The resulting partial charges are shown in Figure 2. All these partial charges correspond to the parameters  $q_i$  in eq 1. The QM/MM method as well as the procedure to determine liquid-phase charges is identical to our

**Table 1.** Density of Water Cosolvent in Simulated ILs<sup>a</sup>

solvent	$\rho_{\text{water}}$ (molecules/nm <sup>3</sup> )
$[\text{C}_4\text{mim}][\text{PF}_6]$	0.92
$[\text{C}_8\text{mim}][\text{PF}_6]$	0.46
$[\text{C}_8\text{mim}][\text{BF}_4]$	3.46

<sup>a</sup> Values are based on measured water saturation concentrations.<sup>44</sup>

previous IL parametrizations, and we refer to ref 45 for a more detailed description.

The same QM/MM procedure was also applied in a recent preceding work to derive partial charges of the solutes TRPc and TRPz in  $[\text{C}_4\text{mim}][\text{BF}_4]$  and  $[\text{C}_4\text{mim}][\text{PF}_6]$ , which are given in Figure 4 of ref 57. The influence of the cation alkyl chain length on the TRP charge polarization was neglected, i.e., the same charges were used for  $[\text{C}_8\text{mim}][\text{BF}_4]$  and  $[\text{C}_8\text{mim}][\text{PF}_6]$ , respectively.

**2.2. Specification of MD Simulations.** All MD simulations were performed with the GROMACS software package.<sup>58</sup> Simulated systems contained 10 TRPc solutes that were solvated with 490 ion pairs of  $[\text{C}_4\text{mim}][\text{PF}_6]$ ,  $[\text{C}_8\text{mim}][\text{BF}_4]$ , and  $[\text{C}_8\text{mim}][\text{PF}_6]$ , respectively, as well as TRPz solvated in 490 ion pairs of  $[\text{C}_4\text{mim}][\text{PF}_6]$ . In systems that contained TRPc, 10 additional anions of the corresponding IL were added to balance the charge. Furthermore, water molecules were added to these simulated systems. In extraction processes, ILs are in direct contact with the water phase over a longer period of time. Thus, water diffuses into the ILs until the saturation concentration is reached. Therefore, the chosen concentrations of added water in the simulations corresponded to the experimentally determined water saturation concentrations in the ILs.<sup>44</sup> At room temperature, the mole fractions of water in saturated  $[\text{C}_4\text{mim}][\text{PF}_6]$ ,  $[\text{C}_8\text{mim}][\text{PF}_6]$ , and  $[\text{C}_8\text{mim}][\text{BF}_4]$  were found to be 0.26, 0.20, and 0.63, respectively, which translated to addition of 168, 113, and 851 water molecules to the simulation systems, respectively.<sup>44</sup> The resulting water densities are given in Table 1. The total number of atoms in simulations ranged from 16 366 to 22 612. The cubic simulation boxes were simulated with full periodic boundary conditions, where all atoms including hydrogen were allowed to move freely without constraints. For nonbonded interactions, a cutoff of 15 Å was used together with fast particle-mesh Ewald electrostatics and dispersion energy corrections to describe long-range interactions.<sup>59–61</sup> All systems were equilibrated in the isothermal–isobaric ensemble (NPT). Temperature and pressure were adjusted with Berendsen coupling using a coupling time constant of 0.1 ps for the thermostat and a coupling constant of 1 ps with a compressibility of  $4.5 \times 10^{-5} \text{ bar}^{-1}$  and a target pressure of 1 atm for the barostat, respectively. An integration step size of 1 fs was used. The translation of the center of mass was removed. Coordinates, velocities, and forces were collected every 2 ps, while energy data was written out every 0.2 ps for data analysis.

All initial simulation box dimensions were chosen so that the solutions were diluted by a factor of about 10 compared to measured densities. Initial close contacts between ions and solutes were removed by minimizing the potential energy with the conjugate gradient method. Subsequently, MD simulations were performed for 10.5 ns. During the first 500 ps all molecules were slowly heated up to 1000 K. The high temperature and low density at the beginning of the simulations facilitated ion mobility massively, which prevented ions from being trapped at local high-energy minima



**Table 2.** Calculated Solvation Free Energies, Measured Partition Coefficients, Solvation Free Energies, Scaling Factors, and Scaled Solvation Free Energies of TRP and Water in Various ILs

solutes + solvent	$\Delta G_{\text{solv}}^{\text{calcd } b}$ [kcal/mol]	$P_{\text{IL}/W}^c$	$\Delta G_{\text{solv}}^{\text{exp } f}$ [kcal/mol]	$s^h$	$\Delta G_{\text{solv}}^{\text{calcd } \cdot s^{bi}}$ [kcal/mol]
TRPc + [C <sub>4</sub> mim][PF <sub>6</sub> ] <sup>a</sup>	−101.5 <sub>4</sub>	0.42 <sup>d</sup>	~−79.6	~0.79	−81.2 <sub>3</sub>
TRPc + [C <sub>8</sub> mim][PF <sub>6</sub> ] <sup>a</sup>	−98.5 <sub>5</sub>	0.02 <sup>d</sup>	>−79.6	<0.81	−78.8 <sub>4</sub>
TRPc + [C <sub>8</sub> mim][BF <sub>4</sub> ] <sup>a</sup>	−103.0 <sub>9</sub>	3.99 <sup>d</sup>	<−79.6	>0.78	−82.3 <sub>8</sub>
TRPz + [C <sub>4</sub> mim][PF <sub>6</sub> ] <sup>a</sup>	−67.6 <sub>6</sub>	0.014 <sup>e</sup>	>−57.6	<0.86	−54.1 <sub>5</sub>
H <sub>2</sub> O + [C <sub>4</sub> mim][PF <sub>6</sub> ]	−4.8	n/a	−3.9 <sup>g</sup>	0.80	−3.8

<sup>a</sup> Water was added according to measured saturation concentrations.<sup>44</sup> <sup>b</sup> Statistical uncertainties of the last digit are given as subscripts. <sup>c</sup> Values were taken from refs 41 and 42. The average was taken in the case of deviating values. <sup>d</sup> Value at pH = 1. <sup>e</sup> Value at pH = 4.16. <sup>f</sup> Derived from eq 7, where the previously reported solvation free energy of TRPc and TRPz in water of −79.6 and −57.6 kcal/mol were inserted, respectively.<sup>57</sup> <sup>g</sup> Value was taken from ref 63. <sup>h</sup> Range of scaling factors for  $\Delta G_{\text{solv}}^{\text{calcd}}$  that would allow reproduction of the corresponding  $\Delta G_{\text{solv}}^{\text{exp}}$ . The relations for  $s$  taken together limit the value to 0.80. <sup>i</sup> Value of  $\Delta G_{\text{solv}}^{\text{calcd}}$  after a scaling with a factor of 0.80.

close to their initial positions. The temperature was maintained at 1000 K for the next 8.5 ns for TRP and water and then subsequently cooled down to 300 K within 1 ns. For the IL solvents the temperature was maintained at 1000 K only for 5 ns and then cooled down to 300 K during the next 4.5 ns. This enabled a fast diffusion of hot solutes to facilitate the finding of energetically favorable positions within the colder solvent during the second half of the simulation. The fast diffusion of solutes in the ILs is beneficial, since diffusivity in ILs is generally very low compared to molecular liquids. In the last step, all molecules were equilibrated for 500 ps at 300 K. The final systems were then used to initialize solvation free energy simulations.

**2.3. Evaluation of Solvation Free Energies.** Thermodynamic integration with MD simulations was used as implemented in GROMACS to calculate solvation free energies of TRP in different ILs. The following potential energy  $E(\lambda)$  was used

$$E(\lambda) = (1 - \lambda)E_{\text{solute+solvent}} + \lambda E_{\text{solvent}} \quad (2)$$

While  $E_{\text{solute+solvent}}$  designates the total potential energy that involves solvent, solute, and solvent–solute interactions,  $E_{\text{solvent}}$  corresponds to the potential energy of the solvent only, where the solute is ignored. During simulations, the coupling parameter  $\lambda$  is stepwise increased from 0 to 1, which corresponds to a successive switching off of the solute–solvent interactions. The free energy difference between the initial state at  $\lambda = 0$  and the final state at  $\lambda = 1$  is the solvation free energy of the solute,  $\Delta G_{\text{solv}}$ , and given by

$$\Delta G_{\text{solv}} = \int \left\langle \frac{\partial E(\lambda_i)}{\partial \lambda} \right\rangle_{\text{MD with } E(\lambda_i)} d\lambda \quad (3)$$

In eq 3,  $\partial E(\lambda_i)/\partial \lambda$  is averaged at each  $\lambda$  point over sample structures that were generated with MD simulations that used the corresponding potential  $E(\lambda_i)$ . The solvation free energy was obtained with numerical integration of eq 3 using Simpson's rule. The solvation free energy can also be written as a sum of Coulomb and Lennard–Jones contributions

$$\Delta G_{\text{solv}} = \Delta G_{\text{solv}}^{\text{Coul}} + \Delta G_{\text{solv}}^{\text{LJ}} \quad (4)$$

While the first term contains contributions from solute–solvent Coulomb interactions, the second term involves solute–solvent van der Waals interactions as well as the energy that is required by solvent reorganization to form the cavity that accommodates the solute.

Solute–solvent interactions were switched off adiabatically in two subsequent steps, where in the first step the Coulomb

contributions were gradually removed and in the second step the Lennard–Jones contributions. A soft-core potential of the following form was used to avoid singularities in the potential at  $\lambda$  close to 1 when short distances between atom pairs are encountered<sup>62</sup>

$$V_{\text{sc}} = (1 - \lambda)V \left[ \left( \alpha \sigma^6 \lambda^P + r^6 \right)^{1/6} \right] \quad (5)$$

$V$  is the normal hard-core potential and  $\alpha$  is the soft-core parameter. In simulations  $\alpha = 0.5$ ,  $\sigma = 3$  Å, and  $P = 1$  were used.

All solvation free energy calculations were initialized with equilibrated TRP–IL structures, as described in the previous section. Spacing between  $\lambda$  points was 0.1; however, finer step widths of 0.05 were used when required. The solute–solvent interactions of all 10 solutes were switched off simultaneously to reduce the involved computational effort, where solvation free energies were obtained as average solvation free energy per solute. This approach is adequate since solute–solute interactions among TRPs could be neglected as demonstrated in ref 57. Simulations of 500 ps length were performed at each  $\lambda$  point using an NVT ensemble, which resulted in total simulation times of 21 ns or longer per system. The statistical uncertainty of  $\Delta G_{\text{solv}}$  was determined with the block averaging technique at each  $\lambda$  point and subsequent error propagation.

### 3. RESULTS AND DISCUSSIONS

**3.1. Calibration of Solvation Free Energy Simulations.** In the first step, calculated solvation free energies of TRP in ILs were compared with experimental data to validate the computational approach. Solvation free energies of amino acids in ILs have not been measured directly; however, a comparison of calculated values of  $\Delta G_{\text{solv}}$  for TRP in ILs could be compared with measured partition coefficients. Partition coefficients of TRP between ILs and aqueous solution,  $P_{\text{IL}/W}$ , are defined as

$$P_{\text{IL}/W} = c_{\text{IL}}/c_W \quad (6)$$

In eq 6,  $c_{\text{IL}}$  and  $c_W$  designate the concentrations of TRP in the IL and the aqueous phase, respectively. The value of  $P_{\text{IL}/W}$  is related to the solvation free energy difference of TRP in the two phases

$$\log P_{\text{IL}/W} = \frac{\Delta G_{\text{solv}}^{\text{TRP}, \text{H}_2\text{O}} - \Delta G_{\text{solv}}^{\text{TRP}, \text{IL}}}{2.303RT} \quad (7)$$

In eq 7,  $\Delta G_{\text{solv}}^{\text{TRP}, \text{H}_2\text{O}}$  and  $\Delta G_{\text{solv}}^{\text{TRP}, \text{IL}}$  are the solvation free energy of TRP in water and the IL, respectively. A direct comparison of calculated values of  $\Delta G_{\text{solv}}^{\text{TRP}, \text{H}_2\text{O}} - \Delta G_{\text{solv}}^{\text{TRP}, \text{IL}}$  and the measured values according to eq 7 is not feasible, however. The protonation

**Table 3.** Calculated Solvation Free Energies, Electrostatic, and Lennard–Jones Contributions of TRP in Various Solvents<sup>a</sup>

solutes + solvent	$\Delta G_{\text{solv}}^{\text{IL}}$	$\Delta G_{\text{solv}}^{\text{Coul}}$	$\Delta G_{\text{solv}}^{\text{LJ}}$
TRPc + [C <sub>4</sub> mim][PF <sub>6</sub> ] <sup>b</sup>	−81.2 <sub>3</sub> (−73.4 <sub>4</sub> )	−74.1 <sub>3</sub> (−65.2 <sub>3</sub> )	−7.1 <sub>1</sub> (−8.2 <sub>2</sub> )
TRPc + [C <sub>8</sub> mim][PF <sub>6</sub> ] <sup>b</sup>	−78.8 <sub>4</sub> (−73.7 <sub>3</sub> )	−70.2 <sub>4</sub> (−65.0 <sub>3</sub> )	−8.6 <sub>1</sub> (−8.7 <sub>1</sub> )
TRPc + [C <sub>8</sub> mim][BF <sub>4</sub> ] <sup>b</sup>	−82.3 <sub>8</sub>	−74.9 <sub>8</sub>	−7.4 <sub>1</sub>
TRPz + [C <sub>4</sub> mim][PF <sub>6</sub> ] <sup>b</sup>	−54.1 <sub>5</sub>	−48.2 <sub>5</sub>	−7.4 <sub>2</sub>
TRPc + H <sub>2</sub> O	−80.0		
TRPz + H <sub>2</sub> O	−58.0		

<sup>a</sup> Solvation free energies were scaled with a factor of 0.80; details are given in section 3.1. All energies are given in kcal/mol. Statistical uncertainties of the last digit are given as subscripts. Values in parentheses were derived from the same IL without water. <sup>b</sup> Water was added according to measured saturation concentrations.<sup>44</sup>

state of TRP in the extraction process is determined by the pH value of the aqueous phase. In measurements, even at a low pH < 1 where cationic TRP vastly dominates,  $P_{\text{IL}/\text{W}}$  did not converge to a specific value, as can be seen, e.g., in Figure 3 of ref 41. Despite this limitation, relations between the solvation free energy of TRP in water and ILs can be derived: at pH < 2.38, where TRPc dominates in the aqueous phase, it can be concluded that  $\Delta G_{\text{solv}}^{\text{TRPc,IL}} < \Delta G_{\text{solv}}^{\text{TRPc,H}_2\text{O}}$  when values of  $P_{\text{IL}/\text{W}}$  are substantially larger than one, whereas for values close to zero  $\Delta G_{\text{solv}}^{\text{TRPc,IL}} > \Delta G_{\text{solv}}^{\text{TRPc,H}_2\text{O}}$ . In cases where  $P_{\text{IL}/\text{W}}$  is close to one, it can be assumed that  $\Delta G_{\text{solv}}^{\text{TRPc,IL}} \approx \Delta G_{\text{solv}}^{\text{TRPc,H}_2\text{O}}$ . Similar conclusions regarding the solvation free energy of TRPz can be made for  $P_{\text{IL}/\text{W}}$  values that were obtained at pH > 2.38, where zwitterionic TRPz dominates.

Experimental  $P_{\text{IL}/\text{W}}$  values for tryptophan<sup>41,42</sup> in the considered ILs are given in Table 2 for reference. For [C<sub>8</sub>mim][PF<sub>6</sub>], a  $P_{\text{IL}/\text{W}}$  value of 0.02 was obtained at pH = 1, i.e., the concentration of TRPc in water was much higher than that in the IL. Thus,  $\Delta G_{\text{solv}}^{\text{TRPc,H}_2\text{O}} < \Delta G_{\text{solv}}^{\text{TRPc,[C}_8\text{mim][PF}_6\text{]}}$ . Extraction with [C<sub>8</sub>mim][BF<sub>4</sub>] was by far more efficient, as indicated by  $P_{\text{IL}/\text{W}} = 3.99$  at pH = 1; therefore,  $\Delta G_{\text{solv}}^{\text{TRPc,H}_2\text{O}} > \Delta G_{\text{solv}}^{\text{TRPc,[C}_8\text{mim][BF}_4\text{]}}$ . Furthermore, with the weaker extractant [C<sub>4</sub>mim][PF<sub>6</sub>] it was found that  $P_{\text{IL}/\text{W}} = 0.42$  at pH = 1, which suggests that values of  $\Delta G_{\text{solv}}^{\text{TRPc,H}_2\text{O}}$  and  $\Delta G_{\text{solv}}^{\text{TRPc,[C}_4\text{mim][PF}_6\text{]}}$  are similar. For the same IL,  $P_{\text{IL}/\text{W}}$  drops to 0.014 at pH = 4.16, i.e.,  $\Delta G_{\text{solv}}^{\text{TRPz,H}_2\text{O}} < \Delta G_{\text{solv}}^{\text{TRPz,[C}_4\text{mim][PF}_6\text{]}}$ .

In Table 2, calculated free solvation energies,  $\Delta G_{\text{solv}}^{\text{calcd}}$ , are compared with experimental solvation free energies,  $\Delta G_{\text{solv}}^{\text{exp}}$ . The value ranges for  $\Delta G_{\text{solv}}^{\text{exp}}$  were derived from the relations given above, where calculated solvation free energies for TRPc and TRPz in water, −79.6 and −57.6 kcal/mol, respectively, were inserted.<sup>57</sup> Measured values for  $\Delta G_{\text{solv}}^{\text{TRP,H}_2\text{O}}$  were not available. A comparison of  $\Delta G_{\text{solv}}^{\text{calcd}}$  and  $\Delta G_{\text{solv}}^{\text{exp}}$  revealed that calculated solvation energies in ILs were substantially overestimated. Two probable reasons for this observed deviation from experimental values were suspected: (1) A lack of equilibration of the IL simulations, where reorganization of the IL is expected to be slow due to low ion diffusivity and pronounced long-range correlations of ion positions. (2) Inaccuracies of the force field, where, e.g., charge transfer between TRP and water has been neglected, could lead to the observed overestimated solvation energies in ILs compared to water solvents. For the system TRPc in [C<sub>4</sub>mim][PF<sub>6</sub>] long simulations were performed with a length of 5 ns per  $\lambda$  point to scrutinize equilibration of the shorter 500 ps simulations. A comparison of the results is given in Figure S1a, Supporting

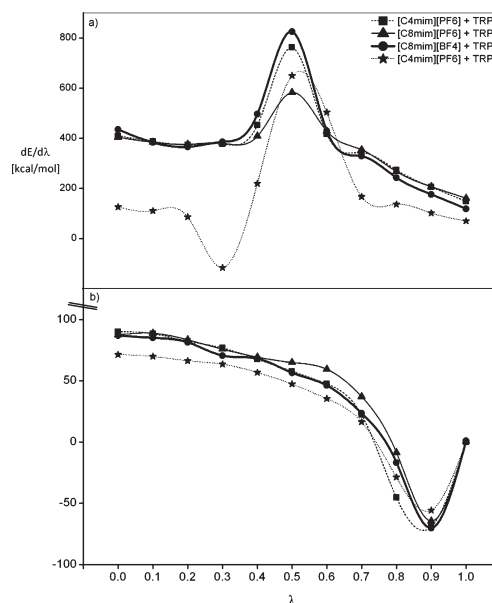


**Figure 3.** Values of  $dE/d\lambda$  as a function of  $\lambda$  for the Coulomb contribution (a) and the Lennard–Jones contribution (b) of TRPc and TRPz in different ILs. Water was added as a cosolvent to all ILs according to measured saturation concentrations. Integrals of these curves were used to determine solvation free energies.

Information. A decrease of 3.0 kcal/mol of the solvation free energy was observed, which could be attributed to the Coulomb contribution. This decrease is compared to the overall deviation from the experiment of about 20 kcal/mol. Furthermore, the solvation free energy of water in the same IL was calculated with long MD simulations; the results are shown in Figure S1b, Supporting Information. For this system, the solvation free energy has been measured directly.<sup>63</sup> An increase of the simulation time to 5 ns length per  $\lambda$  point did not change the simulation result significantly compared to shorter 500 ps simulations. Thus, the remaining deviation of 0.8 kcal/mol from the measured value was not caused by a lack of equilibration. Overall, we concluded that the observed deviation from experimental data is primarily due to limitations of the computational model, but we could also conclude that the simulations of 500 ps length were sufficient to equilibrate the systems.

We introduced a constant scaling factor,  $s$ , for  $\Delta G_{\text{solv}}^{\text{calcd}}$  in ILs to take into account the shortcomings of the computational approach. We like to emphasize that this scaling factor did not affect any of the conclusions in the following sections, which are mostly qualitative. However, a scaling factor facilitated an understanding of the TRP extraction process, which is explained in section 3.4. In any event, the found relations for  $\Delta G_{\text{solv}}^{\text{exp}}$  limited the range of possible values of  $s$  to a single value of 0.80, which is explained in Table 2. Scaled values of  $\Delta G_{\text{solv}}^{\text{calcd}}$  are given in the last column of Table 2. All scaled solvation energies were consistent with measured values of  $P_{\text{IL}/\text{W}}$ , and furthermore, the solvation free energy of water in [C<sub>4</sub>mim][PF<sub>6</sub>] was reproduced as well. In other words, a constant scaling with  $s = 0.80$  reproduced all experimental data correctly. In the following, only scaled solvation free energies are given.

**3.2. Effect of Alkyl Chain Length on TRP Solvation and Impact of Water as Cosolvent.** Initially, TRPc was simulated in [C<sub>4</sub>mim][PF<sub>6</sub>] and [C<sub>8</sub>mim][PF<sub>6</sub>] without water to investigate the influence of the alkyl chain length on liquid–liquid extraction.

**Table 4.** Coordination Numbers of Water and Anions around TRP and Moieties of TRP in Various ILs<sup>a</sup>

solute + solvent	TRPc–H <sub>2</sub> O	TRPc–anion	COO(H)–H <sub>2</sub> O	NH <sub>3</sub> <sup>+</sup> –H <sub>2</sub> O	NH–H <sub>2</sub> O
TRPc + [C <sub>4</sub> mim][PF <sub>6</sub> ]	3.7	5.0	2.2	2.2	0.3
TRPc + [C <sub>8</sub> mim][PF <sub>6</sub> ]	1.0	5.1	0.6	1.0	0.2
TRPc + [C <sub>8</sub> mim][BF <sub>4</sub> ]	6.0	7.8	3.4	3.3	0.6
TRPz + [C <sub>4</sub> mim][PF <sub>6</sub> ]	1.3	2.8	1.5	0.6	0.3

<sup>a</sup> Coordination numbers were derived from an integration of RDFs according to eq 8.

Calculated solvation free energies and contributions from the Coulomb and Lennard–Jones potential are given in Table 3. Surprisingly, the solvation free energy of TRPc in [C<sub>4</sub>mim][PF<sub>6</sub>] was found to be –73.4 kcal/mol, which was not significantly different from the value for TRPc in [C<sub>8</sub>mim][PF<sub>6</sub>]. This seemingly contradicted the observation that extraction of TRPc in [C<sub>8</sub>mim][PF<sub>6</sub>] was found to be less efficient,<sup>41</sup> which suggests the relation  $\Delta G_{\text{solv}}^{\text{TRPc}, [\text{C}_4\text{mim}][\text{PF}_6]} < \Delta G_{\text{solv}}^{\text{TRPc}, [\text{C}_8\text{mim}][\text{PF}_6]}$ . In the next step, water molecules were added to the ILs, according to measured saturation concentrations, which provided a more realistic representation of the IL phase as explained in section 2.2.<sup>44</sup> Water densities in simulated systems are given in Table 1. The water density in [C<sub>4</sub>mim][PF<sub>6</sub>] is 0.92 molecules/nm<sup>3</sup>, which is twice as large as the density in [C<sub>8</sub>mim][PF<sub>6</sub>]. The presence of the hydrophobic octyl side chains in [C<sub>8</sub>mim][PF<sub>6</sub>] prevents a higher water concentration in this IL.

Solvation energies are given in Table 3, where average values of  $dE/d\lambda$  at each  $\lambda$  point are shown in Figure 3. Solvation of TRPc improved substantially in both ILs, where a decrease of the solvation energy of 7.8 and 5.1 kcal/mol was found in [C<sub>4</sub>mim][PF<sub>6</sub>] and [C<sub>8</sub>mim][PF<sub>6</sub>], respectively. In particular, solvation of TRPc in [C<sub>4</sub>mim][PF<sub>6</sub>] with water cosolvent was significantly more favorable than in [C<sub>8</sub>mim][PF<sub>6</sub>], as expected from experiments. While an increase of the alkyl chain length led to a slight decrease of the Lennard–Jones contribution, the Coulomb contribution increased significantly. These findings indicated that the solvation of TRPc in ILs is improved by Coulomb interactions of TRPc with the water cosolvent, which in turn led to the relation  $\Delta G_{\text{solv}}^{\text{TRPc}, [\text{C}_4\text{mim}][\text{PF}_6]} < \Delta G_{\text{solv}}^{\text{TRPc}, [\text{C}_8\text{mim}][\text{PF}_6]}$  in line with the experiment.

The solvation shell around TRPc in the ILs was analyzed in the next step to confirm the role of the water cosolvent. Center of mass radial distribution functions (RDFs) between TRPc or TRPc moieties and anions or water were determined. The number of ions or water molecules that are coordinated to TRPc,  $N$ , were calculated by integrating the corresponding RDF,  $g(r)$ , from 0 to the first minimum,  $r_{\text{min}}$

$$N = 4\pi\rho_0 \int_0^{r_{\text{min}}} g(r)r^2 dr \quad (8)$$

In eq 8,  $\rho_0$  is the ion or water number density in solution. The calculated coordination numbers are given in Table 4 for all simulated ILs.

In [C<sub>4</sub>mim][PF<sub>6</sub>], the number of anions coordinated to TRPc was 5.0, which was hardly affected by the increase of alkyl chain length in [C<sub>8</sub>mim][PF<sub>6</sub>], i.e., octyl, basically did not disrupt the TRPc–anion coordination that was present in [C<sub>4</sub>mim][PF<sub>6</sub>]. The number of water molecules coordinated to TRPc in [C<sub>4</sub>mim][PF<sub>6</sub>] was 3.6, which was substantially higher than in [C<sub>8</sub>mim][PF<sub>6</sub>], where only 1.0 water molecule was found around TRPc. This difference was expected due to the different water densities in the two ILs. These coordination numbers explain why the

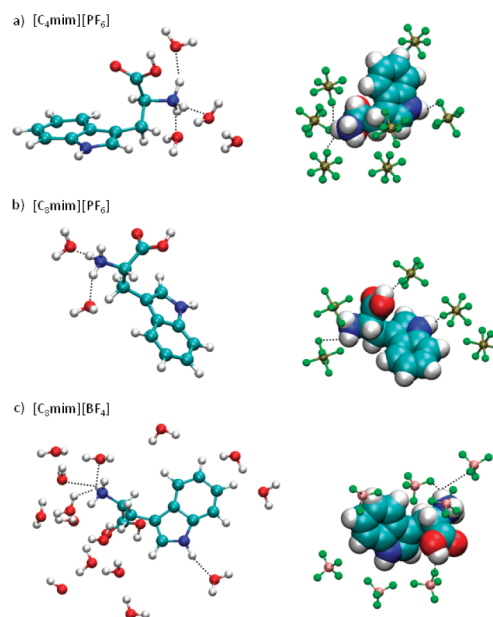


**Figure 4.** Representative sample structures of TRPc solvated in [C<sub>4</sub>mim][PF<sub>6</sub>] (a), [C<sub>8</sub>mim][PF<sub>6</sub>] (b), and [C<sub>8</sub>mim][BF<sub>4</sub>] (c) taken from equilibrated MD simulations. Water and anions within 5 Å of TRPc are displayed on the left-hand and right-hand side, respectively. Hydrogen bonds between TRPc and water or anions are shown as broken lines.

solvation free energy of TRPc is equal in the two ILs without water and why solvation of TRPc in [C<sub>4</sub>mim][PF<sub>6</sub>] is more facilitated than in [C<sub>8</sub>mim][PF<sub>6</sub>] when water as a cosolvent is considered. Furthermore, it was found that water was positioned preferably in the vicinity of the polar –COOH and –NH<sub>3</sub><sup>+</sup> groups, while only a few water molecules were observed near –NH, the third polar group of TRPc. Representative sample structures of TRPc in which water molecules and anions within 5 Å of the solute are shown in Figure 4 for both ILs. Overall, the positions of water close to the polar groups of TRPc were a result of dipole–dipole interactions between water and TRPc, where these additional Coulomb interactions facilitated solvation of TRPc. This effect was less emphasized in [C<sub>8</sub>mim][PF<sub>6</sub>], where hydrophobic octyl prevented diffusion of a larger amount of water into the IL. These findings provide an explanation why ILs that involve long alkyl side chains generally diminish extraction of TRP and other amino acids.<sup>40</sup>

**3.3. Influence of Anion on TRP Solvation.** In this section we examined the role of the anions in the extraction process by comparing the solvation free energies of TRPc in [C<sub>8</sub>mim][PF<sub>6</sub>] and [C<sub>8</sub>mim][BF<sub>4</sub>]. In both cases, the ILs were saturated with water. Solvation free energies are given in Table 3, and average values of  $dE/d\lambda$  at each  $\lambda$  point are shown in Figure 3. Even though both ILs contain the same cations, the water density in



$[\text{C}_8\text{mim}][\text{BF}_4]$  is 7.5 times higher than in  $[\text{C}_8\text{mim}][\text{PF}_6]$  due to the hydrophilic  $\text{BF}_4^-$  anions. It was found that solvation of TRPc in  $[\text{C}_8\text{mim}][\text{BF}_4]$  was more favorable by 3.5 kcal/mol, which is in line with experimental findings. A similar trend has also been observed for other amino acids, such as alanine and lysine, for instance, as well as for different imidazolium-based ILs.<sup>40</sup> A comparison of the contributions to the solvation energies in the two ILs indicated that the improved solvation of TRPc in  $[\text{C}_8\text{mim}][\text{BF}_4]$  stemmed from electrostatic interactions of TRPc with the IL and water as expected. The stronger TRPc–solvent interactions originated from the additional water in the solution, as explained in the previous section. A further reason was the stronger interaction of  $\text{BF}_4^-$  anions with polar TRPc groups, compared to  $\text{PF}_6^-$ , due to the smaller size and stronger charge polarization of the anions.<sup>43</sup> The stronger charge polarization is indicated by the large partial charges on the fluorine atoms of  $-0.51$  e in the case of  $\text{BF}_4^-$  compared to  $-0.39$  e in  $\text{PF}_6^-$ , as can be seen in Figure 2. Overall,  $\text{BF}_4^-$  facilitates extraction of TRPc directly, due to stronger interactions with the solute, as well as indirectly, due to its hydrophilicity that allows an increase of the amount of water around TRPc, which in turn also increases the interaction strength with the solute.

The coordination numbers of anions and water with respect to TRPc or TRPc moieties in  $[\text{C}_8\text{mim}][\text{BF}_4]$  are given in Table 4. The coordination numbers were 7.8 and 6.0 for anions and water, respectively, both of which were considerably higher than in  $[\text{C}_8\text{mim}][\text{PF}_6]$ . Again, water molecules were preferably found near the two most polar groups of TRPc,  $-\text{COOH}$  and  $-\text{NH}_3^+$ . Furthermore, a sample structure of TRPc with surrounding anions and water in  $[\text{C}_8\text{mim}][\text{BF}_4]$  is shown in Figure 4, which illustrates the increased number of anions and water around TRPc. While the increased number of water molecules was simply a result of the large water density in this IL, the larger number of anions around TRPc was caused by the smaller size of  $\text{BF}_4^-$  compared to  $\text{PF}_6^-$ , which led to a higher ion density in the IL as well as due to the stronger interactions of  $\text{BF}_4^-$  with TRPc.

Overall, the results of the previous two sections demonstrated that the water density in the IL, which is determined by the hydrophilicity of cations and anions as well as the capability of anions to participate in strong electrostatic interactions with the solute, primarily determine the effectiveness of the IL as an extractant for amino acids.

**3.4. Analysis of Tryptophan Extraction Process.** The following considerations are based on calculated solvation free energies of TRPc and TRPz in ILs and water, which are listed in Table 3: At  $\text{pH} > 2.34$ , TRP is predominantly zwitterionic in the aqueous phase. Measured values of  $P_{\text{IL}/\text{W}}$  were substantially smaller than one in all considered ILs, i.e., TRPz was not extracted. Indeed, the solvation free energy of TRPz in water was considerably more favorable in water than in  $[\text{C}_4\text{mim}][\text{PF}_6]$ . The transfer free energy of TRPz from water to the IL was  $\Delta G_{\text{trans}}^{\text{wat} \rightarrow \text{IL}} = \Delta G_{\text{solv}}^{\text{IL}} - \Delta G_{\text{solv}}^{\text{wat}} = 4$  kcal/mol. In the aqueous phase, the solvation energy is determined by a balance of favorable dipole–dipole interactions between water molecules and TRPz and an energetically unfavorable formation of a solute cage for TRPz that requires the breaking of hydrogen bonds between water molecules. This solute cage formation energy is expected to be substantially larger in the IL phase, since counterions need to be separated to accommodate the solute. Evidence for large solute cage formation energies in ILs compared to water was reported before for a protein.<sup>64</sup> The larger solute cage formation energy in  $[\text{C}_4\text{mim}][\text{PF}_6]$  might have been partially compensated by stronger solute–solvent interactions, where TRPz interacts with

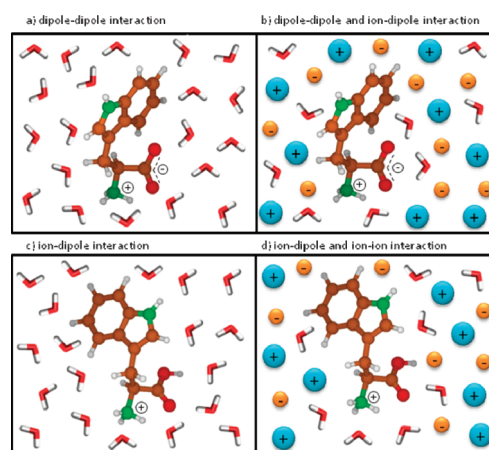


**Figure 5.** Schematic representation of types of interactions that occur when zwitterionic TRP is solvated in water (a) and ILs (b) as well as when cationic TRP is solvated in water (c) and ILs (d). Polar groups of TRPz interact with the dipoles of water (dipole–dipole) and ions (dipole–ion) in the ILs. In the case of TRPc, interactions with water and ions can be described as ion–dipole and ion–ion interactions, respectively. The water cosolvent in ILs adds further dipole–dipole and ion–dipole interactions with TRPz and TRPc, respectively.

ions as well as with dipoles from the water cosolvent. In any event, the overall result is a weaker solvation of TRPz in the IL.

At  $\text{pH} < 2.34$ , TRP is protonated and becomes cationic TRPc. For this compound,  $P_{\text{IL}/\text{W}}$  varied over a large range of values, depending on the composition of the ILs. The smallest  $P_{\text{IL}/\text{W}}$  value was measured in  $[\text{C}_8\text{mim}][\text{PF}_6]$ , where TRPc could not be extracted. Solvation of TRPc in water was indeed more favorable than in this IL, with  $\Delta G_{\text{trans}}^{\text{wat} \rightarrow \text{IL}} = 1.2$  kcal/mol. According to this result, even the stronger ion–ion interactions between TRPc and the IL ions were not sufficient to compensate for the large solute cage formation energy. Only when a sufficient amount of water was solvated in the IL phase, due to more hydrophilic cations, such as in  $[\text{C}_4\text{mim}][\text{PF}_6]$ , the additional dipole–dipole interactions between water and TRPc tipped the balance in favor of the IL phase, so that TRPc could be extracted. Indeed, the calculated value of  $\Delta G_{\text{trans}}^{\text{wat} \rightarrow \text{IL}}$  was  $-1.2$  kcal/mol. The largest value of  $P_{\text{IL}/\text{W}}$  was found in  $[\text{C}_8\text{mim}][\text{BF}_4]$ , where an even larger amount of water was present in the IL phase. Additionally, the  $\text{BF}_4^-$  anions increased the TRPc–IL interaction strength directly, which both substantially enhanced the extraction of TRPc. It should be expected, however, that this effect was partially compensated by an impeded solute cage formation due to stronger ion–ion interactions in the IL. The calculated value of  $\Delta G_{\text{trans}}^{\text{wat} \rightarrow \text{IL}}$  was  $-2.3$  kcal/mol. A possibly further increase of  $P_{\text{IL}/\text{W}}$  with  $[\text{C}_4\text{mim}][\text{BF}_4]$  cannot be achieved, since this IL is water miscible and would not form a biphasic system with water. The occurring interactions between TRP and the solvents are schematically shown in Figure 5.

Furthermore, transfer free energies for the transfer of TRPc between two ILs were compared with measured values. According to eq 7 it can be derived

$$\Delta G_{\text{trans}}^{\text{IL}_1 \rightarrow \text{IL}_2} = RT \ln(P_{\text{IL}_1/\text{W}}/P_{\text{IL}_2/\text{W}}) = \Delta G_{\text{solv}}^{\text{IL}_2} - \Delta G_{\text{solv}}^{\text{IL}_1} \quad (9)$$

Values of  $P_{\text{IL}/\text{W}}$  were considered at  $\text{pH} = 1$ , which is close to the lowest pH value for which data was available, which ensured that

**Table 5. Measured and Calculated Transfer Free Energies for Transfer of TRPc between Different ILs<sup>a</sup>**

IL <sub>1</sub> → IL <sub>2</sub>	$\Delta G_{\text{trans}}^{\text{IL},\text{exp } b}$	$\Delta G_{\text{trans}}^{\text{IL},\text{calcd}}$
[C <sub>4</sub> mim][PF <sub>6</sub> ] → [C <sub>8</sub> mim][PF <sub>6</sub> ]	1.8	2.4
[C <sub>8</sub> mim][BF <sub>4</sub> ] → [C <sub>8</sub> mim][PF <sub>6</sub> ]	3.2	3.5
[C <sub>8</sub> mim][BF <sub>4</sub> ] → [C <sub>4</sub> mim][PF <sub>6</sub> ]	1.2	1.1

<sup>a</sup> All energies are given in kcal/mol. <sup>b</sup> Values were derived with eq 9 with values for  $P_{\text{IL}/\text{W}}$  at pH = 1 that were taken from refs 41 and 42. An average  $P_{\text{IL}/\text{W}}$  was used in the case of deviating values. The transfer free energies depend on the pH of the aqueous phase.

the vast majority of TRP in the biphasic systems were in their cationic form. The results are given in Table 5. All calculated values were in good agreement with experimental data, which suggests that calculated relative solvation free energies of TRP in different ILs were reproduced adequately. However, it needs to be kept in mind that measured values of  $\Delta G_{\text{trans}}^{\text{IL},\text{exp}}$  at a pH lower than one would somewhat deviate from the values in Table 5, which limits the validity of the comparison.

The reason for the strong pH dependency of measured  $P_{\text{IL}/\text{W}}$  values at a very low pH could be explained with an ion-exchange mechanism.<sup>40,41</sup> For each TRPc that is transferred from the aqueous phase to the IL charge neutrality requires that one cation from the IL needs to diffuse into the aqueous phase. Thus, extraction of TRPc is limited by the ability of the aqueous phase to accommodate cations from the IL. At low pH, the concentration of protons becomes comparable with the concentration of TRPc in the aqueous phase, so that the partition of TRPc, proton–water complexes, and IL cations between the two phases will mutually affect each other. In any event, further investigations are required to clarify the strong pH dependency of measured  $P_{\text{IL}/\text{W}}$ .

Overall, the results of this work suggest that extraction of TRP and other amino acids can be achieved with ILs that contain ions that are sufficiently hydrophilic to increase the water saturation concentration in the IL phase, as long as the IL remains water immiscible. Furthermore, small anions with large dipole moments improve the extraction further, due to stronger ion–solute interactions. It should be taken into account, however, that hydrophilic ILs are also more difficult to recycle, since these ILs are more soluble in the water phase.

#### 4. CONCLUSION

Extraction of TRP from aqueous solutions with the ILs [C<sub>4</sub>mim][PF<sub>6</sub>], [C<sub>8</sub>mim][PF<sub>6</sub>], and [C<sub>8</sub>mim][BF<sub>4</sub>] was analyzed by determining the solvation free energies of cationic and zwitterionic TRP in these ILs with MD simulations. A comparison with solvation free energies that were derived from the previously reported partition of TRP between ILs and water indicated that solvation of TRP was overestimated in simulations. Thus, a constant scaling factor of 0.80 was introduced for calculated solvation free energies, with which all experimental data could be reproduced, including transfer free energies of TRP for transfer between two ILs.

Reduced solvation of TRPc in [C<sub>8</sub>mim][PF<sub>6</sub>] compared to [C<sub>4</sub>mim][PF<sub>6</sub>] was reproduced in calculations correctly when the ILs were saturated with water, which was the case in the actual extraction experiments. No differences in solvation free energies of TRPc were obtained however when water in the ILs was removed, which demonstrated the importance of water in ILs for amino acid extraction. The water cosolvent facilitated TRP solvation

by 8 and 5 kcal/mol in [C<sub>4</sub>mim][PF<sub>6</sub>] and [C<sub>8</sub>mim][PF<sub>6</sub>], respectively. In [C<sub>8</sub>mim][PF<sub>6</sub>], the hydrophobic octyl groups limited diffusion of water into the IL phase, thereby reducing favorable electrostatic interactions of TRPc with water dipoles compared to [C<sub>4</sub>mim][PF<sub>6</sub>], which in turn impedes TRP extraction.

Furthermore, the particular importance of anions in the extraction process was confirmed by finding a substantially improved solvation of TRPc in [C<sub>8</sub>mim][BF<sub>4</sub>] compared to [C<sub>8</sub>mim][PF<sub>6</sub>] by 3.4 kcal/mol, which is in line with experimental observations. BF<sub>4</sub><sup>−</sup> anions are more hydrophilic than PF<sub>6</sub><sup>−</sup>, which led to a larger water concentration in the IL phase and to more water molecules in the vicinity of TRPc in the IL. As a result, electrostatic interactions between TRPc and solvent intensified, which facilitated solvation of TRPc. Additionally, the localized anion charge on the more compact BF<sub>4</sub><sup>−</sup> and its larger charge polarization enabled stronger direct electrostatic interactions with TRPc, which facilitated the extraction process further.

Overall, the hydrophilicity of IL constituting ions determines the water concentration in the IL phase, where higher concentrations facilitated solvation of TRPc and thus its extraction from the aqueous phase. Hydrophilic ions are typically characterized by large partial charges on atoms that participate in hydrogen bonds with water, whose magnitude depends on the charge polarization of the groups that constitute the ions.

In this work, the impact of anions and cation alkyl chain length on extraction of TRP was elucidated and the importance of water as a cosolvent of ILs was identified. We expect that these results also apply qualitatively to extraction of other amino acids.

#### ■ ASSOCIATED CONTENT

**S Supporting Information.** Values of the Coulomb contribution to  $\langle \partial E(\lambda) / \partial \lambda \rangle$  for water and TRPc in the IL [C<sub>4</sub>mim][PF<sub>6</sub>], respectively, were derived from MD simulations of 5 ns length per  $\lambda$  point and compared to corresponding values of shorter simulations. This material is available free of charge via the Internet at <http://pubs.acs.org>.

#### ■ AUTHOR INFORMATION

##### Corresponding Author

\*Phone: (49) 89 289 13766. E-mail: marco.klaehn@tum.de.

#### ■ ACKNOWLEDGMENT

We acknowledge gratefully the provision of computing facilities by the Institute of High Performance Computing (IHPC) and financial support from the Agency for Science, Technology and Research (A\*STAR) of Singapore.

#### ■ REFERENCES

- (1) Perry, F. G. Biotechnology in animal feeds and animal feeding: an overview. In *Biotechnology in animal feeds and animal feeding*; Wallace, J. R., Chesson, A., Eds.; Wiley-VCH: Weinheim, Germany, 1995; pp 1–17.
- (2) Dajanta, K.; Apichartsrangkoon, A.; Chuksatitrot, E.; Frazier, R. A. *Food Chem.* **2011**, *125*, 342.
- (3) Barbul, A.; Lazarou, S. A.; Efron, D. T.; Wasserkrug, H. L.; Efron, G. *Surgery* **1990**, *108*, 331.
- (4) Ziegler, T. R.; Young, L. S.; Benfell, K.; Scheltinga, M.; Hortos, K.; Bye, R.; Morrow, F. D.; Jacobs, D. O.; Smith, R. J.; Antin, J. H.; Wilmore, D. W. *Ann. Intern. Med.* **1992**, *116*, 821.



- (5) Cascaval, D.; Oniscu, C.; Galaction, A. I. *Biochem. Eng. J.* **2001**, *7*, 171.
- (6) Juang, R. S.; Wang, Y. Y. *J. Membr. Sci.* **2002**, *207*, 241.
- (7) Lo, T. C. *Handbook of Separation Techniques for Chemical Engineers*; McGraw-Hill: New York, 1996.
- (8) Martinez-Aragon, M.; Burghoff, S.; Goetheer, E. L. V.; de Haan, A. B. *Sep. Purif. Technol.* **2009**, *65*, 65.
- (9) Aoyama, Y.; Asakawa, M.; Yamagishi, A.; Toi, H.; Ogoshi, H. *J. Am. Chem. Soc.* **1990**, *112*, 3145.
- (10) Chen, H.; Ogo, S.; Fish, R. H. *J. Am. Chem. Soc.* **1996**, *118*, 4993.
- (11) Hano, T.; Matsumoto, M.; Ohtake, T.; Sasaki, K.; Hori, F.; Kawano, Y. *J. Chem. Eng. Jpn.* **1990**, *23*, 734.
- (12) Kelly, N. A.; Lukhezo, M.; Reuben, B. G.; Dunne, L. J.; Verrall, M. S. *J. Chem. Technol. Biotechnol.* **1998**, *72*, 347.
- (13) Lipkowitz, K. B.; Raghothama, S.; Yang, J. *J. Am. Chem. Soc.* **1992**, *114*, 1554.
- (14) Molinari, R.; De Bartolo, L.; Drioli, E. *J. Membr. Sci.* **1992**, *73*, 203.
- (15) Wieczorek, P.; Jonsson, J. A.; Mathiasson, L. *Anal. Chim. Acta* **1997**, *346*, 191.
- (16) Zheng, J. Y.; Konishi, K.; Aida, T. *Tetrahedron* **1997**, *53*, 9115.
- (17) Smirnova, S. V.; Torocheshnikova, I. I.; Pletnev, I. V. *Russ. Chem. Bull.* **2000**, *49*, 952.
- (18) Park, S.; Kazlauskas, R. J. *Curr. Opin. Biotechnol.* **2003**, *14*, 432.
- (19) Rogers, R. D.; Seddon, K. R. *Science* **2003**, *302*, 792.
- (20) Seddon, K. R. *Nat. Mater.* **2003**, *2*, 363.
- (21) Wasserscheid, P.; Keim, W. *Angew. Chem., Int. Ed.* **2000**, *39*, 3773.
- (22) Wasserscheid, P.; Welton, T. *Ionic Liquids in Synthesis*; Wiley-VCH: Weinheim, 2003.
- (23) Welton, T. *Chem. Rev.* **1999**, *99*, 2071.
- (24) Huddleston, J. G.; Willauer, H. D.; Swatloski, R. P.; Visser, A. E.; Rogers, R. D. *Chem. Commun.* **1998**, 1765.
- (25) Branco, L. C.; Crespo, J. G.; Afonso, C. A. M. *Angew. Chem., Int. Ed.* **2002**, *41*, 2771.
- (26) Branco, L. C.; Crespo, J. G.; Afonso, C. A. M. *Chem.—Eur. J.* **2002**, *8*, 3865.
- (27) Esser, J.; Wasserscheid, P.; Jess, A. *Green Chem.* **2004**, *6*, 316.
- (28) Fadeev, A. G.; Meagher, M. M. *Chem. Commun.* **2001**, 295.
- (29) Gutowski, K. E.; Broker, G. A.; Willauer, H. D.; Huddleston, J. G.; Swatloski, R. P.; Holbrey, J. D.; Rogers, R. D. *J. Am. Chem. Soc.* **2003**, *125*, 6632.
- (30) He, C. Y.; Li, S. H.; Liu, H. W.; Li, K.; Liu, F. *J. Chromatogr. A* **2005**, *1082*, 143.
- (31) Holbrey, J. D.; Visser, A. E.; Spear, S. K.; Reichert, W. M.; Swatloski, R. P.; Broker, G. A.; Rogers, R. D. *Green Chem.* **2003**, *5*, 129.
- (32) Li, S. H.; He, C. Y.; Liu, H. W.; Li, K.; Liu, F. *J. Chromatogr. B* **2005**, *826*, 58.
- (33) Liu, Q. F.; Yu, J.; Li, W. L.; Hu, X. S.; Xia, H. S.; Liu, H. Z.; Yang, P. *Sep. Sci. Technol.* **2006**, *41*, 2849.
- (34) Smirnova, S. V.; Torocheshnikova, I. I.; Formanovsky, A. A.; Pletnev, I. V. *Anal. Bioanal. Chem.* **2004**, *378*, 1369.
- (35) Soto, A.; Arce, A.; Khoshkbarchi, M. K. *Sep. Purif. Technol.* **2005**, *44*, 242.
- (36) Visser, A. E.; Swatloski, R. P.; Reichert, W. M.; Mayton, R.; Sheff, S.; Wierzbicki, A.; Davis, J. H.; Rogers, R. D. *Chem. Commun.* **2001**, 135.
- (37) Visser, A. E.; Swatloski, R. P.; Rogers, R. D. *Green Chem.* **2000**, *2*, 1.
- (38) Zhang, J. M.; Zhang, Y. Q.; Chen, Y. H.; Zhang, S. J. *J. Chem. Eng. Data* **2007**, *52*, 2488.
- (39) Zhao, H.; Xia, S. Q.; Ma, P. S. *J. Chem. Technol. Biotechnol.* **2005**, *80*, 1089.
- (40) Absalan, G.; Akhond, M.; Sheikhan, L. *Amino Acids* **2010**, *39*, 167.
- (41) Tome, L. I. N.; Catambas, V. R.; Teles, A. R. R.; Freire, M. G.; Marrucho, I. M.; Coutinho, J. A. P. *Sep. Purif. Technol.* **2010**, *72*, 167.
- (42) Wang, J.; Pei, Y.; Zhao, Y.; Hu, Z. *Green Chem.* **2005**, *7*, 196.
- (43) Klähn, M.; Stüber, C.; Seduraman, A.; Wu, P. *J. Phys. Chem. B* **2010**, *114*, 2856.
- (44) Freire, M. G.; Neves, C. M. S. S.; Carvalho, P. J.; Gardas, R. L.; Fernandes, A. M.; Marrucho, I. M.; Santos, L. M. N. B. F.; Coutinho, J. A. P. *J. Phys. Chem. B* **2007**, *111*, 13082.
- (45) Klähn, M.; Seduraman, A.; Wu, P. *J. Phys. Chem. B* **2008**, *112*, 10989.
- (46) Lopes, J. N. C.; Padua, A. A. H.; Shimizu, K. *J. Phys. Chem. B* **2008**, *112*, 5039.
- (47) Sorin, E. J.; Pande, V. S. *Biophys. J.* **2005**, *88*, 2472.
- (48) Mahoney, M. W.; Jorgensen, W. L. *J. Chem. Phys.* **2000**, *112*, 8910.
- (49) Mahoney, M. W.; Jorgensen, W. L. *J. Chem. Phys.* **2001**, *114*, 363.
- (50) Jorgensen, W. L.; Chandrasekhar, J.; Madura, J. D.; Impey, R. W.; Klein, M. L. *J. Chem. Phys.* **1983**, *79*, 926.
- (51) Chaumont, A.; Schurhammer, R.; Wipff, G. *J. Phys. Chem. B* **2005**, *109*, 18964.
- (52) Klähn, M.; Seduraman, A.; Wu, P. *J. Phys. Chem. B* **2008**, *112*, 13849.
- (53) Frisch, M. J.; Trucks, G. W.; Schlegel, H. B.; Scuseria, G. E.; Robb, M. A.; Cheeseman, J. R.; Montgomery, J. A., Jr.; Vreven, T.; Kudin, K. N.; Burant, J. C. *Gaussian 03*, Revision C.02; Gaussian, Inc.: Wallingford, CT, 2004.
- (54) Becke, A. D. *J. Chem. Phys.* **1993**, *98*, 5648.
- (55) Lee, C. T.; Yang, W. T.; Parr, R. G. *Phys. Rev. B* **1988**, *37*, 785.
- (56) Breneman, C. M.; Wiberg, K. B. *J. Comput. Chem.* **1990**, *11*, 361.
- (57) Klähn, M.; Seduraman, A.; Wu, P. *J. Phys. Chem. B* **2011**, *115*, 8231.
- (58) Van der Spoel, D.; Lindahl, E.; Hess, B.; Groenhof, G.; Mark, A. E.; Berendsen, H. J. C. *J. Comput. Chem.* **2005**, *26*, 1701.
- (59) Allen, M. P.; Tildesley, D. J. *Computer simulations of liquids*; Oxford Science Publications: Oxford, 1987.
- (60) Darden, T.; York, D.; Pedersen, L. *J. Chem. Phys.* **1993**, *98*, 10089.
- (61) Essmann, U.; Perera, L.; Berkowitz, M. L.; Darden, T.; Lee, H.; Pedersen, L. G. *J. Chem. Phys.* **1995**, *103*, 8577.
- (62) Shirts, M. R.; Pitera, J. W.; Swope, W. C.; Pande, V. S. *J. Chem. Phys.* **2003**, *119*, 5740.
- (63) Anthony, J. L.; Maginn, E. J.; Brennecke, J. F. *J. Phys. Chem. B* **2001**, *105*, 10942.
- (64) Klähn, M.; Lim, G. S.; Seduraman, A.; Wu, P. *Phys. Chem. Chem. Phys.* **2011**, *13*, 1649.